

Finite Element Method analysis of the deformation of the shaft and supports of a large, precise lathe – Cutting force excitation

Stanislau Dounar¹, Alexandre Iakimovitch¹, Andrzej Jakubowski²✉

¹ Belarusian National Technical University, Mechanical Engineering Faculty
Nezalezhnasci 65, 220127 Minsk, Belarus

² Maritime University of Szczecin, Faculty of Marine Engineering
1–2 Waly Chrobrego St., 70-500 Szczecin, Poland
e-mail: a.jakubowski@am.szczecin.pl
✉ corresponding author

Key words: FEA, lathe, rotor, centerline, excitation, resonance

Abstract

In this paper, Finite Element Method (FEA) harmonic analysis of the changes caused by raising the centerline of a large, precise lathe is presented. Two standalone dynamic subsystems (“Rotor Shaft” and “Support”) are revealed and the resilience of the “Rotor Shaft” to the raising procedure is stated. The three subsystems of the “Support” class are much more dynamically pliable, only the main eigenmodes of the shaft and supports are excited in the 0...100 Hz range (MR1 “Half-wave” and MS1...3 “Radial pecking”). Mounting the lunette suppresses the MR1 peak by a factor of two; therefore the lunette is strongly recommended, with an optional tuned-mass damper (TMD). The support’s resonant frequencies MS1...3 are more deleterious for precision; they should be omitted or weakened using TMD’s that are attached to the supports. For the above conditions, raising the centerline (up to 600 mm) may be included in the lathe renovation program.

Introduction

The dynamic behavior of a large, precise lathe is discussed in this paper. Such a lathe should be appropriate for both rough turning and precision turning. Bulky forged or cast shafts can be completely machined by a single machine tool with tolerances as small as $\pm 10 \mu\text{m}$. This is common practice for the production of propulsion shafts and rotors destined for ship energy transmissions, hydropower plants, etc.

Presented here is the second part of the investigation about a specific lathe FEA simulation. The first part (Dounar et al., 2018) was devoted to static deformation and the eigenmodes. Therefore, the FEA-model and the boundary conditions were inherited from that article. A similar model was developed (Vasilevich & Dounar, 2017) for the centerless kind

of turning using the same lathe. Stock experience using the simulation was gained for a range of heavy machine tools (Vasilevich, Dounar & Karabaniuk, 2016).

Herein the lathe was loaded using harmonic testing forces in the frequency range of 0 to 100 Hz. The forces cause the lathe to deform in the radial direction, which is critical for machining precision; resonance excitations and the governing factors are the focus here.

The centerline raising procedure (CRP) was planned during the non-usual renovation of the lathe. Centerline refers to the common axis of the spindle, tailstock quill and the turned workpiece. Raising the centerline by 0, 300, 600 mm should be evaluated; these height grades will be referred to below as IHL, RHL and EHL. As the machine tool becomes taller, the dynamic swaying of the structural parts may

become deleterious for precision (Tobias, 1965; Stepan et al., 2017). The aim of the present work is to investigate the acceptable level of raising the centerline from a dynamic point of view. CRP up to the height $h = 600$ mm would increase the maximal diameter of cutting from $\phi 2150$ to $\phi 3350$ mm. Therefore, extra-large rotor shafts could be turned after renovation of the lathe.

Dynamic simulation of the lathe

Figure 1 shows a typical rotor shaft, Sh, to be machined (for a large generator or turbine) being held at the front by the chuck Ch and the spindle Sp (incorporated in the headstock HS) and by quill Q of the tailstock TS at the back. A section of the bed Bd and multiple feet Ft are visible. The shaft should be turned

or milled in the assembly with the rotor Rt ($\phi 2250$ mm) and the hydrostatic bearings RB and AB.

The rise in the centerline's height is equal to $h = 600$ mm in the case for EHL. The shaft is swinging at a frequency of $f_{MR1} = 13.36$ Hz of the main (lower) eigenmode MR1. The shaft oscillates in accordance with the classic scheme "Half-wave" with nodes $n1, n2$ out of the shaft's space. A single antinode $a1$ is positioned between the rotor Rt and the neighboring bearing RB.

There are up to three supports (Figure 2) S1, S2, S3 (front, middle, and rear) on the guides G1...G4 of the lathe bed. Every support holds a tool (generalized; $t1, t2, t3$ – mill cutter). The vertex of any tool may be loaded during simulation of the radial force. For example, force F2 acts from tool $t2$ (Figure 2) to the opposite side on the shaft.

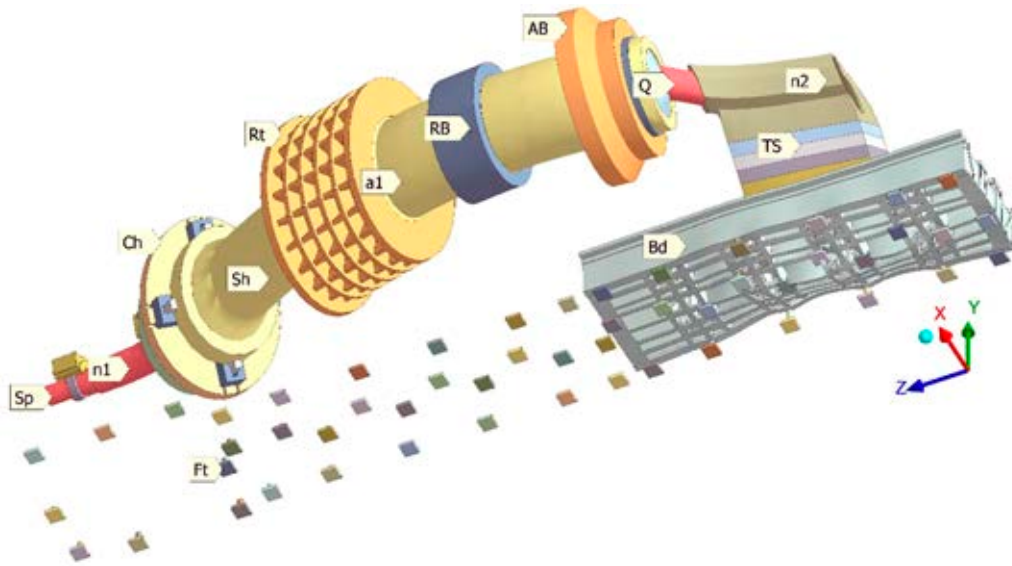


Figure 1. Main resonance of the machined shaft Sh – M1 "Half-wave" (13.36 Hz) – for the case of raising the centerline by 600 mm: $n1, n2$ – end nodes; $a1$ – single antinode (lathe parts are mostly hidden; bottom view; EHL, $h = 600$ mm)

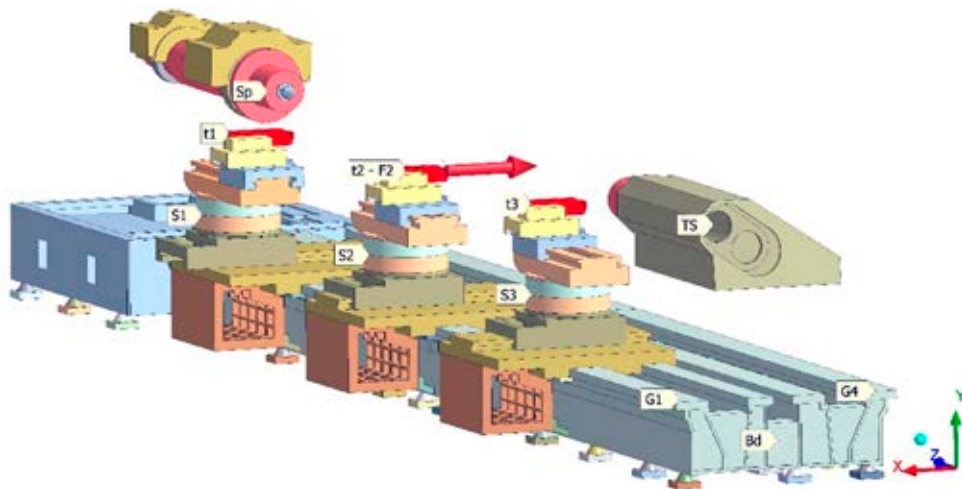


Figure 2. Three supports S1, S2, S3 with tools $t1, t2, t3$: radial force (F2) aimed at the shaft (hidden); centerline is created by spindle Sp and TS axis; RHL, $h = 300$ mm

FEA simulation conditions

The mechanical properties of the simulated materials were assigned in the first part of the investigation. The FEA of the lathe's initial state, developed in conjunction with workshop floor tests, was described in the literature (Dounar et al., 2017). This allowed for the possibility of assigning a vertical rigidity of 3700 N/ μm for every foot below the bed. The horizontal foot rigidity was significantly lower – 1050 N/ μm ; this was tuned by variations in the foot shape/material.

The FEA model is linear; only contact pairs of *bonded* and *no separation* states were applied. Contact openings during cutting force loading were not expected anywhere along the bed guideways due to the high weight of the supports. The radial movements of the tools were controlled by rigid upper drives, simulated as springs. Therefore, the supports and tailstocks were taken as being fixed on the bed by bonded contact pairs.

The lathe's spindle was held at the forward position by a legacy two-row roller bearing (outer diameter – $\phi 680$ mm). The bearing possesses high static radial rigidity (6570 N/ μm), but a very low angular rigidity (due to the bearing's narrowness). This resulted in an effective radial rigidity of only 860 N/ μm (due to the spindle end bending).

The aforementioned rigidity value is sufficient in practice; thus, it is mainly governed by the spindle's bending stiffness. The forward bearing behaves like a type of spherical joint inside the headstock. The forward bearing unit should be reinforced for better angular rigidity; however, this entails a full headstock unit redesign and therefore will not be discussed here.

Herein, three pairs of reference points r_1-t_1 , r_2-t_2 , r_3-t_3 (for the shaft and the tools) are described. Three twin forces, F_1 , F_2 , F_3 , could be applied to the paired points to simulate the cutting process. Each twin force consists of two radial (X) forces, which are opposite direction and equal in value. For example, the twin force F_3 include the component forces F_3^t and F_3^r , acting on the shaft and the tool, respectively.

Both components of the twin force oscillate during the harmonic analysis, trying to engage-disengage the shaft and tool. For example, the components of the twin force F_3 are equal to:

$$F_3^t = A \cdot \sin(2\pi f_{\text{sim}} t), \quad F_3^r = A \cdot \sin(2\pi f_{\text{sim}} t - \pi) \quad (1)$$

where: $A = 1000$ N – constant force amplitude; f_{sim} – excitation frequency for the current simulation, Hz; t – time, s.

The value of amplitude A is not the principal one, because the FEA model is linear and scalable. The dynamic radial stiffness (rigidity) of the support i is the relation of the force amplitude to the displacement in the tool vertex t_i along axis X:

$$J_{S_i}^{d \text{ sim}} = \frac{A}{u_i^t}, \quad \text{N}/\mu\text{m} \quad (2)$$

The radial rigidity of the shaft is calculated in a similar way:

$$J_{r_j}^{d \text{ sim}} = \frac{A}{u_j^r}, \quad \text{N}/\mu\text{m} \quad (3)$$

where: u_i^t – displacement along X for reference point t_i ; u_j^r – displacement along X for reference point r_j .

The dynamic rigidity of both the supports and the shaft depends on the simulation frequency f_{sim} . The dynamic rigidity of any reference point should not be lower than the limit $J_{\text{lim}}^d = 20$ N/ μm (Lopez de Lacalle & Lamikiz, 2008). First of all, this concerns resonance excitation; rough cutting auto-oscillations (mainly, regenerative chatter) (Olvera et al., 2012; Jafarzadeh & Movahhedy, 2017) have a high probability of occurring if the dynamic rigidity of the shaft or the support drops below 5 N/ μm .

The cutting force, for example, F_2 in Figure 2, may oscillate during machining in a wide indefinite frequency range. If its frequency matches the eigenmode frequency of the support or the shaft it is called “frequency overriding”. The very essential question for any machine tool is – which resonant frequencies are “overriding” acceptable for? This depends on the capacity of a given resonance to be excited by a given force. Calculating the dynamic rigidity is necessary here.

The natural damping of the oscillations is taken into account by providing the damping ratio ζ . The damping ratio was assigned (Vasilevich, Dounar & Karabaniuk, 2016; Vasilevich & Dounar, 2017) as being equal to $\zeta_{ci} = 2\%$ for the cast iron that is used for the structural parts. The steel parts – the assembled shaft, spindle, chuck, quill, etc. – have a material damping ratio of $\zeta_{st} = 1\%$. Additionally, the damping ratio $\zeta_{bg} = 1\%$ was assigned to all of the FEA-models to damp background vibration. Tuned mass dampers (TMD) (Yang, Liu & Wang, 2010) were not simulated in the present work.

Excitability of the eigenmodes for the rotor shaft

Previous modal FEA-analysis has revealed that every radial resonance of the lathe at frequencies of

up to 100 Hz is tied to one of two dynamic subsystems. Those subsystems are named:

- “RotorShaft” including a shaft with a headstock, tailstock, and lunette (if present);
- “Support”, consisting of any of support with the tool and flexible bed guides below (there are three such subsystems by the quantity of the supports).

Resonant oscillations never affect the entire lathe, but only one of its dynamic subsystems; this is a valuable feature of machine tool dynamics.

The main, bending “RotorShaft” eigenmode has been shown in Figure 1. The next eigenmode M2 “Wave” is revealed (Figure 3) at twice the higher frequency. That is the bending oscillation of the “RotorShaft” subsystem with a full sinusoidal period pattern. There are 3 nodes and 2 antinodes; the lunette L counteracts antinode a2 near the rear end of the shaft. This region looks like it is prone to vibration. It may be appropriate to mount the second lunette near the chuck in the vicinity of antinode a1.

During the simulation, both resonant frequencies MR1 and MR2 were excited precisely at their

frequencies by the twin forces F_1, F_2, F_3 (pure frequency overriding). Swinging pairs of forces were applied in turns on the related paired points $r_1-t_1, r_2-t_2, r_3-t_3$. There were three factors that were varied – height rise h , presence of the lunette (NoL–WithL) and switching *on* or *off* of the bond between the tool and the shaft (WithB–NoB). The last factor shows a very mean influence. The results of the shaft excitation through the tool t_1 are shown in Table 1.

The following conclusions could be drawn from the data in Table 1:

- The frequencies MR1, MR2 were both very stable for any variations of the factors;
- The resonant MR1 amplitudes at all of the shaft reference points are nearly unaffected by the height rise h ; cells (1, 4), (2, 4), (3, 4) contain nearly the same data, as do (1...3, 5), (1...3, 6); thus the subsystem “RotorShaft” is resilient to changes in the CRP;
- The eigenmode MR2 is excited ten times less than MR1 (compare cells ((3, 4–6) to (7, 4–6));

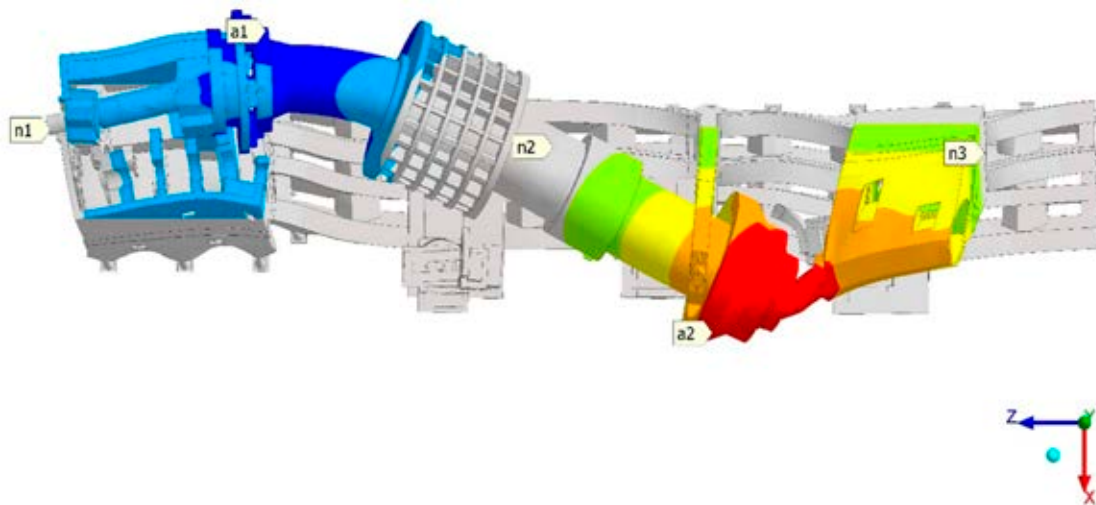


Figure 3. The rotor shaft’s eigenmode MR2 “Wave” (full sinusoidal period; 32.15 Hz) the view from above: n1, n2, n3 – nodes; a1, a2 – antinodes

Table 1. Rotor shaft’s resonant excitation by twin force F_1 through support S1

#	Height rise h , mm	Eigenmode	Natural frequency f_i , Hz	The amplitude at the shaft points, μm			Lunette
				r_1	r_2	r_3	
	1	2	3	4	5	6	7
1	0 (IHL)	MR1	15.00	30.66	36.63	29.94	NoL
2	300 (RHL)	MR1	14.15	31.03	38.59	34.24	NoL
3	600 (EHL)	MR1	13.27	31.14	40.32	38.43	NoL
4	300 (RHL)	MR1	17.26	18.47	20.39	16.99	WithL
5	0 (IHL)	MR2	33.97	3.50	1.91	7.02	NoL
6	300 (RHL)	MR2	31.58	3.79	1.64	7.05	NoL
7	600 (EHL)	MR2	29.34	4.16	1.43	7.20	NoL
8	300 (RHL)	MR2	32.59	2.47	1.77	5.96	WithL

the lathe's precision is mainly threatened by the excitement of MR1;

- The lunette's presence (change from NoL to WithL) alleviates MR1 swinging by a factor of two (cells (4, 4–6) contains levels of 49–59% level compared to (2, 4–6)); the lunette is the agent that can be used to compensate over and above the effect of raising the centerline on the rotor shaft.

The shaft's dynamic rigidity at frequency MR1 is stable during CRP and is kept within the range of $J_{r1}^{dMR1} = 32.1 \dots 32.6 \text{ N}/\mu\text{m}$. Machining at this frequency, overriding resonance MR1, is permitted (but not recommended) because the minimal rigidity is lower ($J_{nom}^d = 20 \text{ N}/\mu\text{m}$). The dynamics of the rotor shaft appears to be resilient to raising the centerline.

Main support resonance excitement

The raised, tower-like supports were rocked in turns by the twin forces at precisely its resonant frequencies (Figure 4; the second situation of frequency overriding). Opposite radial forces were applied at the points t_1-r_1 to support both S1 and the shaft (Figure 4a). Figure 4b shows support S3 and the shaft both swinging due to the similar action at

points t_3-r_3 . The eigenmodes of MS1, MS2, MS3 of the "Radial pecking" class were excited. The natural frequencies differed slightly, as each support in Figure 4 has its own machining diameter.

Figure 4a shows only support S1 swaying. Forced swaying of support S3 is visible in Figure 4b; it can be seen that support S2 also sways without a force being applied. It is likely that support S2 plays the role of a TMD with regard to S3 resonance oscillations.

Excitation of the eigenmodes (MSxx type) was accomplished for the three supports S1, S2, S3 at the three levels of height rise, IHL, RHL and EHL; the results are shown in Table 2. The last line of the table shows the percentage changes in the frequency and the amplitude changing when the centerline rises from IHL to EHL. CRP moderately reduces the resonant frequencies (~80% of the level is preserved). At the same time, all of the amplitudes of the supports were doubled. As the height of the support increased, its radial dynamic rigidity diminished (Figure 5) in a predictable way. In the EHL state, the lathe possesses a stiffness of $8.8 \text{ N}/\mu\text{m}$ for only the tower-like support S1 being at its main resonant frequency; this was 2.3 times less than that of the initial IHL-support.

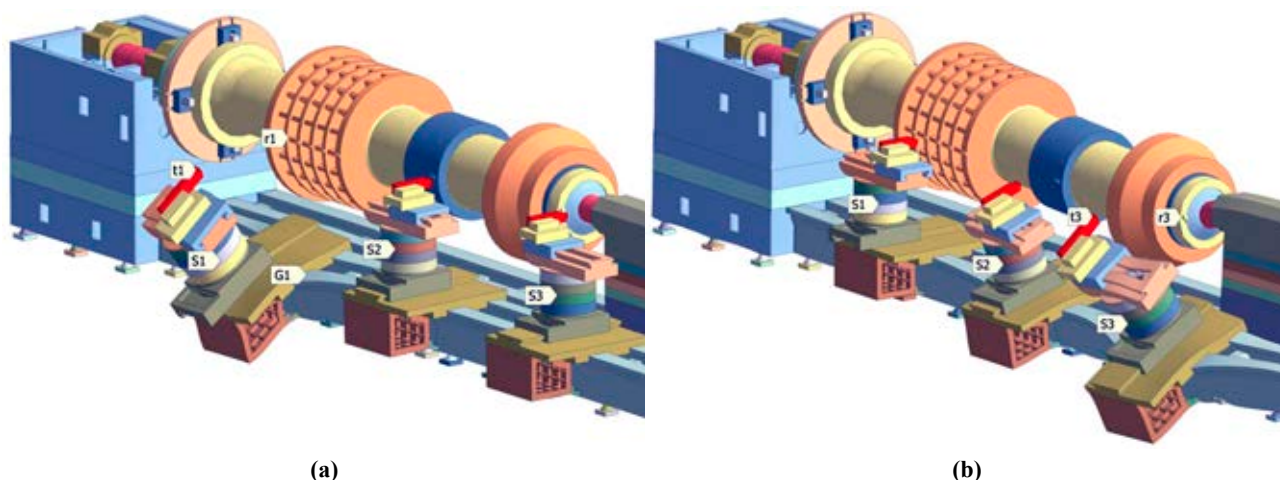


Figure 4. "Radial pecking" resonance excitations for elevated supports S1 (a) and S3 (b) (EHL; $h = 600 \text{ mm}$) at the similar frequencies 42.7 Hz (a; MS1) and 53.6 Hz (a; MS3)

Table 2. Influence of the height rise h on the excitation of resonant frequencies of the supports

#	Height rise h , mm	Eigenmodes MSxx, their frequencies f_{MSxx} (Hz) and amplitudes A_{MSxx} (μm) at the tool's vertexes						Features
		MS1, F_1		MS2, F_2		MS3, F_3		
		f_{MS1}	A_{MS1}	f_{MS2}	A_{MS2}	f_{MS3}	A_{MS3}	
		2	3	4	5	6	7	8
1	0 (IHL)	55.4	48.9	70.0	30.0	65.9	32.08	NoL, NoB
2	300 (RHL)	48.9	76.4	62.5	45.7	59.7	47.13	NoL, NoB
3	600 (EHL)	42.7	112.9	54.9	66.6	53.6	61.49	NoL, NoB
		77%	230%	78%	222%	81%	191%	

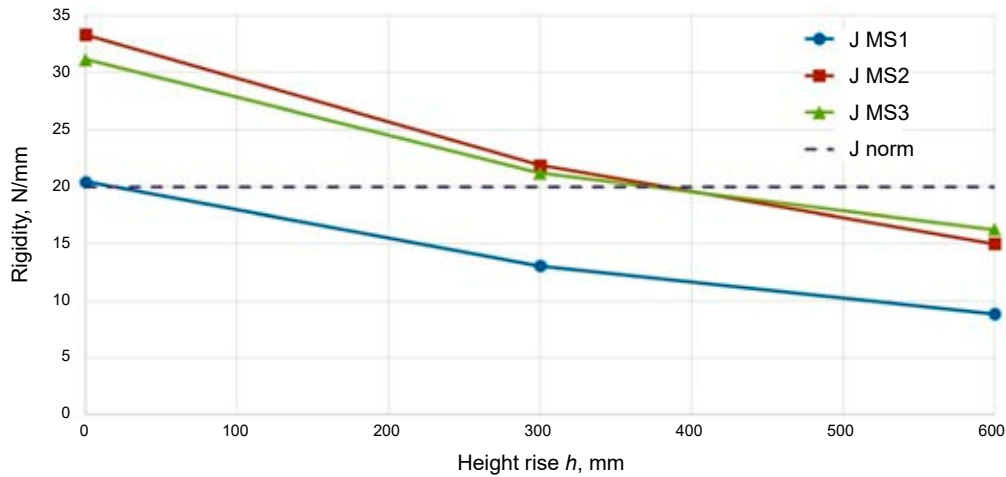


Figure 5. The influence of height rise h on the dynamic rigidity of supports S1, S2, S3 (curves 'J MS1', 'J MS2', 'J MS3') at resonant frequencies MS1, MS2, MS3. 'J norm' shows the limit of rigidity

The rigidity curves should be above the limit line 'J norm', otherwise, descending into auto-oscillation is possible. Therefore, the overriding MSxx resonances are dangerous for all of the supports in the EHL case. For a moderate centerline rise (RHL), overriding is permissible for only the middle and rear supports (S2, S3). The forwards support S1 should not be loaded by an oscillating resonant force in any case. Passive or active damping and machining frequency bypassing are both recommended (Muhammad et al., 2017).

Raising the supports up to 600 mm is appropriate if the "Radial pecking" resonant frequencies are omitted during machining. A rise in the centerline of 300 mm allows turning and milling by tools on supports S2 and S3 at MSxx frequencies. Support S1 creates the most excitable dynamic subsystem;

this is due to its larger machining diameter and its distance from the other supports (weak dynamic damping).

Harmonic analysis and FRFs

Figure 6 depicts the rotor shaft's FRFs, simulated for the case of the middle twin forces, applied to points t_2 and r_2 on support S2 and the shaft, respectively. Curves 'h0', 'h300', and 'h600' relate to the lathe's states of IHL, RHL and EHL (without lunette). Curve 'h300 NoL WithB' differs from 'h300', accounting for the tangential bond 'tool – cutting zone on shaft'. The lunette was additionally simulated and considered (curve 'h300 WithL WithB').

The frequency below ~ 10 Hz relates to the static, pre-resonant range. All of the resonant peaks on the

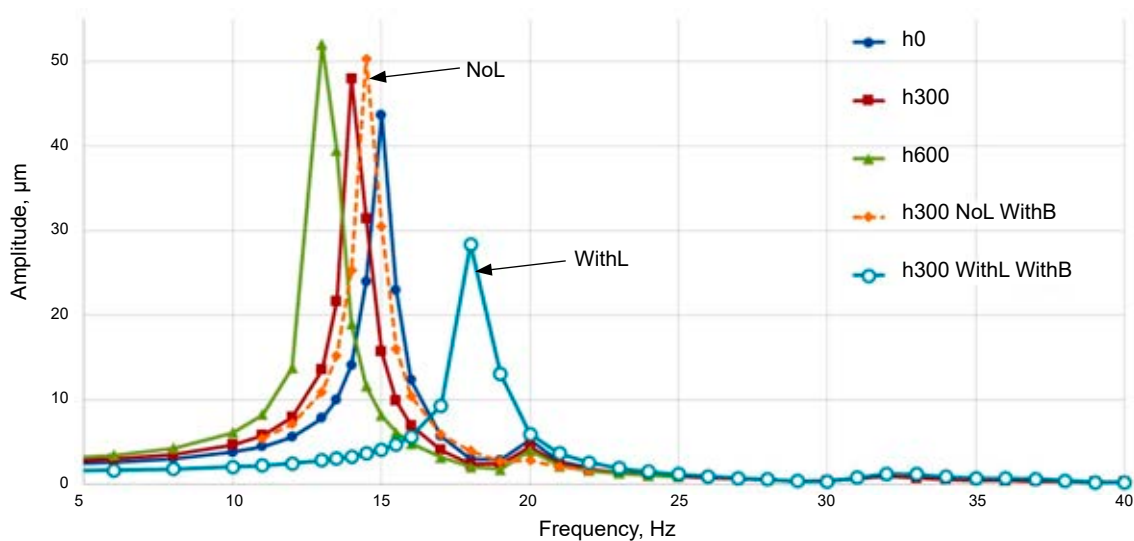


Figure 6. Rotor shaft's FRFs for different height rise h : entry – twin force component for point r_2 ; exit – radial displacement amplitude

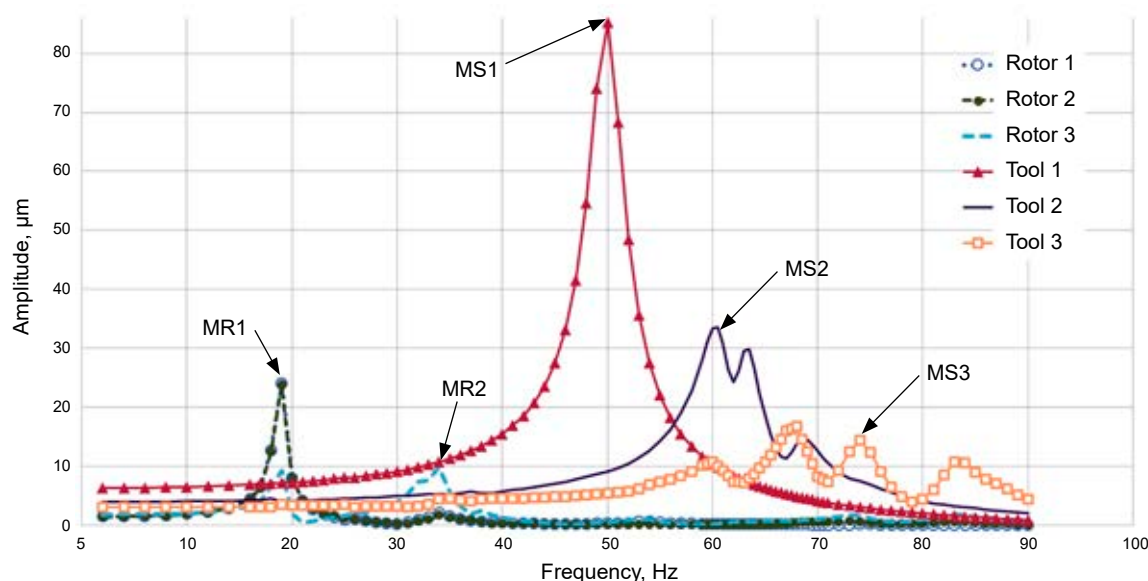


Figure 7. FRFs for points r_1, r_2, r_3 on the rotor shaft and the tool vertexes t_1, t_2, t_3 on the supports; RHL

FRF belong to the MR1 “Half-wave” mode. Most of the peaks lie very close to each other (13...16 Hz) and have nearly the same height. This effect confirms the conclusion about the robustness of the “RotorShaft” subsystem with regard to raising the centerline. The influence of mounting the lunette on the FRF is much stronger. The peak on the curve ‘h300 WithL WithB’ is reduced by a factor of two and shifted up by 5 Hz. The post-resonant range of the shaft begins above ~ 20 Hz.

The tangential bond between the shaft and the tool is not the leading factor; this is indicated by the vicinity of the curves ‘h300’ and ‘h300 NoL WithB’. Raising the lathe is permissible for the rotor shaft’s dynamics. Mounting the lunette and damping allows machining at the cutting frequencies near to the MR1 frequency.

Two FRF clusters are shown in Figure 7. The curves ‘Rotor...’ concern the reference points r_1, r_2, r_3 on the shaft. The twin force components F_1^r, F_2^r, F_3^r serve as the entries and the amplitudes at the same points are the exits. Curves ‘Tool...’ are stack to the tool points t_1, t_2, t_3 amplitudes and the force components F_1^t, F_2^t, F_3^t .

Curves ‘Rotor 1’ and ‘Rotor 2’ nearly coincide; the peak of the rotor resonance MR1 “Half-wave” is visible. The resonance MR2 “Wave” shows itself on the ‘Rotor 3’ curve because the loading point r_3 is located near the antinode of that mode.

The amplitudes of the rotor’s resonances are small in comparison with the supports’ resonances. The most powerful one is the resonance MS1 of the forward support. This is due to the large machining diameter ($\phi 2090$ mm) caused by the high pliability.

At the same time, the peak MS1 is very isolated; this is not reflected in the other FRFs in Figure 7.

Discussion

The rotor shaft’s resonances only slightly affect the support’s FRF and vice versa. Thus, the dynamic subsystems “RotorShaft” and “Supports” have minimal interactions; this is advisable because the resonances MRxx and MSxx should not reinforce each other.

Each resonance MS2 and MS3 induce several peaks in the FRF (Figure 7). This is indicative of the dynamic interplay between the group of supports as well as between the supports, the lunette and the tailstock. Spontaneous coordination of the eigenmodes is typical for large machine tools. The supports, the lunette, and the tailstock act as a TMD for each other. The task of optimization is to tune such unprompted dynamic dampers (Lu et al., 2018).

The position of support S1 is an issue for the lathe’s dynamic pattern; this subsystem is isolated and no dynamic cooperation is observed. For a centerline rise of 600 mm, the support S1 needs frequency controllable loading and additional damping.

Conclusions

A rotor shaft with a headstock and tailstock creates a separate dynamic subsystem inside the lathe that was investigated in this paper. Every raised support with bed guides forms the other subsystem.

Only the main resonances “Half-wave” (shaft) and “Radial pecking” (supports) are dangerously excited by radial cutting forces in the range up to 100 Hz.

The subsystem “RotorShaft” is almost unaffected, and resistant to a rise in the centerline. Mounting the lunette is recommended for the rear part of the shaft; a tuned mass damper (TMD) may also be attached. As for the shaft, machining is allowable with the “overriding” frequency of “Half-wave” resonance even for the maximal rise height $h = 600$ mm (EHL).

The dynamic stiffness of the supports at their resonant frequencies falls during CRP to ~ 9 N/ μ m. The related frequencies should be omitted for an EHL lathe, e.g. by using spindle speed correction. Moderate dynamic interaction between the raised supports has been revealed in the FRFs. This has provided the possibility of using the neighboring supports as TMDs for each other.

The lathe generally possesses resilience to a rise in the centerline, especially the “RotorShaft” subsystem. CRP is possible from a dynamic point of view up to a height of 600 mm. The supports, standing at the maximal machining diameters, should be protected from frequency overriding; omitting excitation and TMD damping are both appropriate.

References

1. DOUNAR, S., IAKIMOVITCH, A., AUSIYEVICH, A. & JAKUBOWSKI, A. (2018) FEA-analysis of shaft and supports deformations for huge precise lathe. Statics and resonances. *New trends in productive engineering* 1, 1, pp. 341–348.
2. DOUNAR, S.S., SOKOROV, I.O., ERMALOVICH, V.I. & MOT-SUK, E.A. (2017) Renovation order analysis for huge lathe by FEA simulation. Part 1. Statics and dynamics of radial direction. *Mashinostroenie: Repub. interdepart. collection of the scientific works proceed.* Vol. 30, Minsk: BNTU, pp. 75–86.
3. JAFARZADEH, E. & MOVAHHEDY, M.R. (2017) Numerical simulation of interaction of mode coupling and regenerative chatter in machining. *Journal of Manufacturing Processes* 27, pp. 252–260.
4. LÓPEZ DE LACALLE, L.N. & LAMIKIZ, A. (2008) *Machine Tools for High Performance Machining.* London: Springer-Verlag.
5. LU, K., LIAN, Z., GU, F. & LIU, H. (2018) Model-based chatter stability prediction and detection for the turning of the flexible workpiece. *Mechanical Systems and Signal Processing* 100, pp. 814–826.
6. MUHAMMAD, B.B., WAN, M., FENG, J. & ZHANG, W. (2017) Dynamic damping of machining vibration: a review. *International Journal of Advanced Manufacturing Technology* 89 (9), pp. 2935–2952.
7. OLVERA, D., LÓPEZ DE LACALLE, L.N., COMPEÁN, F.I., FZ-VALDIVIELSO, A. & CAMPA, F.J. (2012) Analysis of tool tip radial stiffness of turn-milling centers. *International Journal of Advanced Manufacturing Technologies* 60, pp. 883–891.
8. STEPAN, G., KISS, A.K., GHALAHAMCHI, B., SOPANEN, J. & BACHRATHY, D. (2017) Chatter avoidance in cutting highly flexible workpieces. *CIRP Annals* 66 (1), pp. 377–380.
9. TOBIAS, S.A. (1965) *Machine-tool vibration.* London: Blackie & Sons Ltd.
10. VASILEVICH, YU.V., DOUNAR, S.S. & KARABANIUK, I.A. (2016) Finite element analysis of filler influence on dynamic rigidity of heavy machine tool portal. *Science & Technique* 15, 3, pp. 233–241.
11. VASILEVICH, YU.V. & DOUNAR, S.S. (2017) Finite element analysis of centerless-lunette turning of the heavy shaft. *Science & Technique* 16, 3, pp. 196–205.
12. YANG, Y., LIU, Q. & WANG, M. (2010) Optimization of the tuned-mass damper for chatter suppression in turning. *Chinese Journal of Mechanical Engineering* 23 (6), pp. 717–724.